Norwegian Meteorological Institute
met.no

met.no report

no. 6/2012
Climate

# Assessing the suitability of weather generators based on Generalised Linear Models for downscaling climate projections

Lukas Gudmundsson

Norwegian Meteorological Institute
met.no

# report

| Title | Date |
|---|---|
| Assessing the suitability of weather generators based on Generalised Linear Models for downscaling climate projections | March 23, 2012 |
| **Section** | **Report no.** |
| Climate | 6/2012 |
| **Author** | **Classification** |
| Lukas Gudmundsson | ● Free ○ Restricted |
| | **ISSN 1503-8025** |
| **Client(s)** | **Client's reference** |
| Statkraft, Meteorologisk Institutt | MIST |


**Abstract**

This study investigated the potential of conditional weather generators based on Generalised Linear Models for downscaling climate model simulations. The weather generators where trained to model precipitation and temperature in seven catchments in western Norway using free atmosphere variables from the NCEP/NCAR reanalysis. The weather generators capture the seasonal cycle, monthly residuals and the inter annual variability of precipitation and temperature well. As weather generators are often used to provide input for hydrological modelling it is crucial that they also produce a realistic day to day variability. In this context, the ability to capture the short term persistence (measured using autocorrelation) is promising. However, the stochastic nature of weather generators does not permit an interpretation of single events and issues regarding the magnitude of extreme precipitation were observed. The suitability of weather generators for hydrological modelling thus depends on the specific needs of each study and has to be evaluated on a case to case basis. Finally, the trained weather generators were used to downscale simulations from the HadCM3 climate model for different emission scenarios. The results suggest an increase of temperature and a shift in the seasonality of precipitation toward wetter conditions in late summer and fall.



**Keywords**

climate, precipitation, downscaling, GCM, weather generator


| Disciplinary signature | Responsible signature |
|---|---|
| Torill Engen Skaugen | Øystein Hov |


**Postal address** P.O Box 43 Blindern N-0313 OSLO Norway
**Office** Niels Henrik Abels vei 40
**Telephone** +47 2296 3000
**Telefax** +47 2296 3050
**e-mail:** met.inst@met.no **Internet:** met.no
**Bank account** 7694 05 00601
**Swift code** DNBANOKK

# 1 Introduction

Global Climate Models (GCM) and Regional Climate Models (RCM) resolve atmospheric processes on relatively coarse grids, usually covering hundreds or thousands of square kilometres. Consequently these models cannot resolve local weather phenomena such as high precipitation rates due to orographic effects, temperature changes with altitude, or inversions that are confined to narrow valleys. This coarse resolution is contrasted by the need to assess the effects of climate change locally, for example with respect to hydrological applications or crop production. One approach to solve these issues would be to increase the resolution of GCMs or RCMs. Unfortunately such an increase in resolution is to date often not feasible due to limited computational resources.

A popular approach to bridge the gap between the coarse resolution of climate models and the need for local interpretation of climate change is the use of *statistical downscaling* methods. Statistical downscaling refers to a broad class of methods that are used to approximate local weather and climate as a function of large-scale atmospheric characteristics (e.g. pressure fields which are resolved by GCM) using statistical techniques. These techniques are described by a large body of literature, which has been summarised with respect to theoretical considerations and end user needs in a series of comprehensive reviews (Fowler et al., 2007; Maraun et al., 2010; Winkler et al., 2011b,a).

*Conditional weather generators* are receiving increasing attention as downscaling tools that can resolve day to day variability of near surface variables such as precipitation and temperature (e.g. Maraun et al., 2010; Wilks and Wilby, 1999). Weather generators are statistical simulators that produce random numbers with properties resembling those of observed atmospheric variables (Wilks and Wilby, 1999). In their basic form, weather generators do not have any connection to large-scale predictors and are thus not suitable for downscaling. However, weather generators can be constructed to take the temporal variability of large-scale predictors into account, in which case they are referred to conditional weather generators. Conditional weather generators differ from many other statistical downscaling techniques by the use of statistical simulations. The simulation procedure implies that the target variable is not described by one single realisation, but by a large number of possible realisations. Each of these has to be assumed to be highly uncertain, but collectively the simulations can provide robust estimates of the target variables. A large number of conditional weather generators have been proposed, differing in their assumptions as well as in their theoretical and technical complexity (see Maraun et al., 2010; Wilks and Wilby, 1999, and references therein). Among the most popular approaches are simple weather generators that assume that the variable of interest can be described by a linear (regression) model including a first order autoregressive (Markov) component (e.g. Furrer and Katz, 2007; Wilby et al., 1999; Hessami et al., 2008; Wilks and Wilby, 1999). These have been recently extended to incorporate modern statistical estimation techniques, including ridge regression (Hessami et al., 2008) and generalised linear models (Furrer and Katz, 2007; Fealy and Sweeney, 2007).

This study aims at assessing the potential of Generalised Linear Models (GLM) based weather generators to downscale free atmosphere variables to daily precipitation and temperature. After introducing the technical details, the models are trained using observation based estimates of surface variables and free-atmosphere predictors originating from the NCEP/NCAR reanalysis data set. This is followed by a careful assessment of the weather generators ability to capture the variability of observed precipitation and temperature. Finally, the weather generator is used to assess climate change as projected by the HadCM3 climate model. Here the HadCM3 is used as an typical example for the many climate scenarios that require downscaling for climate impact assessment at the local scale.

# 2 A weather generator based on generalised linear models (glm)

The formulation of the weather generators for precipitation and temperature follows closely the work of Furrer and Katz (2007) and Fealy and Sweeney (2007). In a first step the expected value of the variables of interest is modelled as a function of free-atmospheric variables using Generalised Linear Models (GLM). GLM are an extension of linear regression models that incorporate a nonlinear transformation of the response variable. The GLM is identified using maximum likelihood methods, incorporating assumptions on the distribution of the variable of interest. In this study, variable selection is done using stepwise regression, optimising Akaike Information Criterion (AIC). After model identification the GLM can be used to provide daily varying parameters to weather generators.

## 2.1 Precipitation

Daily precipitation is modelled using two independent processes, one for the probability of precipitation occurrence (i.e. whether it rains on a day or not) and one for the precipitation intensity (i.e. the amount of water precipitated).

### 2.1.1 Precipitation Occurrence

Precipitation occurrence at time $t$ is described using an indicator variable, $I_t$, where $I_t = 1$ denotes rainfall and $I_t = 0$ denotes a dry day. Precipitation occurrence is assumed to depend on the precipitation occurrence of the previous day ($I_{t-1}$) i.e. it is a Markov process. Assuming that $I_t$ follows a Bernoulli process, the probability of precipitation occurrence ($p_t$) can be modelled using logistic regression as

$$\ln\left(\frac{p_t}{1-p_t}\right) = \alpha_1 + \alpha_2 I_{t-1} + \sum_{i=1}^{N} \beta_i Y_{t,i}, \tag{1}$$

where $\alpha_1$ is the intercept and $\alpha_2$ the coefficient of the first order autoregressive component, $Y_{t,i}$ are the $N$ free atmosphere variables and $\beta_i$ are the corresponding parameters.

After the occurrence model (Eq. 1) is identified, it can be used to simulate precipitation occurrence as

$$\tilde{I}_t \sim \mathcal{B}(p = p_t), \tag{2}$$

where $\mathcal{B}$ is the Bernoulli distribution with probability $p$ and $\tilde{I}_t$ denotes simulated precipitation occurrence. The occurrence probability for each time step, $p_t$, is obtained by solving Eq. 1.

### 2.1.2 Precipitation Intensity

Precipitation intensity, $\mu_t$, is only defined for wet days ($I_t = 1$) and assumed to be Gamma distributed. The expected value of the logarithm of $\mu_t$ is modelled as

$$\ln(\mu_t) = \alpha_1 + \sum_{i=1}^{N} \beta_i Y_{t,i}. \tag{3}$$

Once identified, the intensity model can be used to simulate the precipitation intensity as

$$\tilde{\mu}_t \sim \Gamma(\kappa = k, \theta = \mu_t/\kappa), \tag{4}$$

where $\Gamma$ is the Gamma distribution with shape parameter $\kappa$ and scale parameter $\theta$. The shape parameter is estimated from observed precipitation intensities using maximum likelihood methods (Furrer and Katz, 2007). The scale parameter is used to account for the expected precipitation intensity $\mu_t$, exploiting the fact that the mean of gamma distributed variables is defined as $\mu = \theta\kappa$.

## 2.2 Temperature

Temperature, $T_t$, is assumed to follow a first order autoregressive process with normal distributed residuals. The deterministic component is modelled as

$$T_t = \alpha_1 + \alpha_2 T_{t-1} + \sum_{i=1}^{N} \beta_i Y_{t,i}. \tag{5}$$

Daily temperature is finally simulated as

$$\tilde{T_t} \sim T_t + \mathcal{N}(\mu = 0, \sigma = \sigma_R), \tag{6}$$

where $\mathcal{N}$ is the normal distribution with zero mean. The standard deviation $\sigma$ is set to $\sigma_R$, the standard deviation of the residuals of Eq. 5.

# 3 Data

## 3.1 Near surface variables

Daily precipitation and temperature for the 1/1/1961 - 31/12/1989 control period where obtained from high resolution (1 km grids) interpolations of observations, which are available for entire Norway at `www.eklima.no`. The variables where obtained for all grid-points in seven selected catchments in western Norway (Figure 1) and their spatial average was used to construct representative time series.

## 3.2 Atmospheric forcing variables

The atmospheric forcing variables (Table 1) where obtained from the SDSM data archive[1] (Wilby and Dawson, 2007), which provides easy access to atmospheric reanalysis and climate model simulations. In this study the NCEP/NCAR atmospheric reanalysis and model simulations of the HadCM3 climate model (A2 and B2 scenarios) where used. All data in the SDSM data archive are normalised over the 1961-1990 period. The atmospheric fields of the SDSM data archive originate from different data sources and are interpolated to the same grid with 2.5° latitude × 3.75° longitude resolution. Only data from the grid-cell at 77.5°N and 11.25°E, which covers the selected catchments (Figure 1) were considered in this study. All data where considered for the 1/1/1961 - 31/12/1989 control period. In addition, the simulations of the HadCM3 model where analysed for the 1/1/2071 - 31/12/2099 scenario period.

To assure that HadCM3 model reproduces the climate of the considered grid-cell reliably, the monthly climatology of the HadCM3 simulations were correlated to the climatology of the NCEP/NCAR reanalysis (Table 2), using the square of Pearson's correlation coefficient ($r^2$). The model reproduces the grid-cell climatology well in most instances. In some cases, however, the correlations are low, indicating considerable uncertainties in the HadCM3 simulations. To reduce the impact of such uncertainties, only variables with $r^2 \geq 0.5$ where considered for further analysis.

[1] `http://cccsn.ca/?page=dst-sdi`, last accessed 31/12/2011

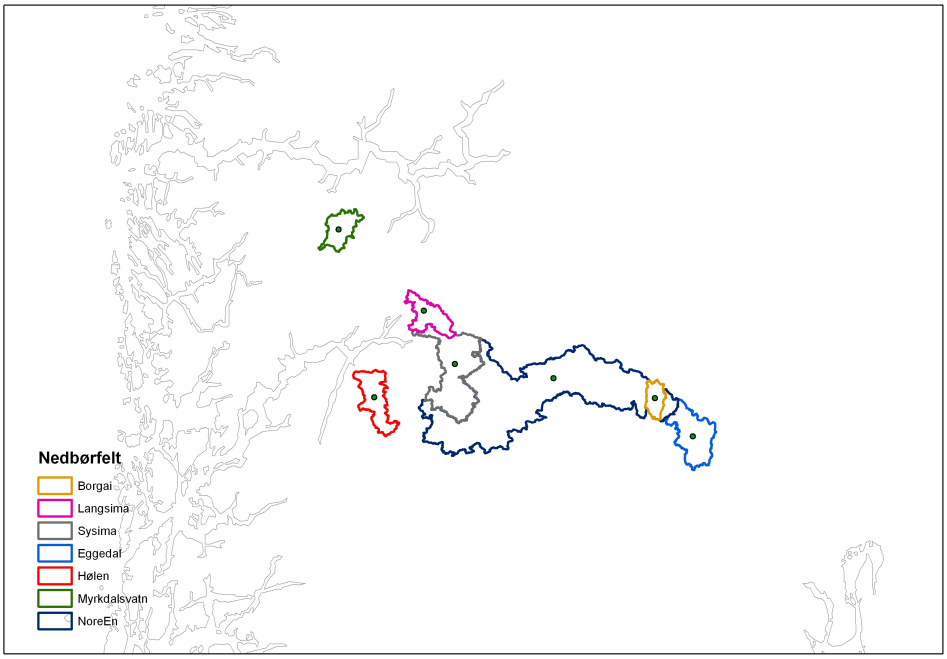


*Figure 1:* Catchments considered in this study

*Table 1:* Candidate predictor variables available from the SDSM data archive (Wilby and Dawson, 2007). *Italics* indicates that the variables have been estimated using geostrophic approximation (** is substituted with p5 for 500 hPa and with p8 for 850 hPa). **Bold** indicates that the variables have not been normalised. (See also `http://cccsn.ca/?page=pred-help` (last accessed: 2/1/2012), for more details.)

| Variable | Code |
|---|---|
| Mean temperature at 2m | temp |
| Mean sea level pressure | mslp |
| 500 hPa geopotential height | p500 |
| 850 hPa geopotential height | p850 |
| Near surface relative humidity | rhum |
| Relative humidity at 500 hPa height | r500 |
| Relative humidity at 850 hPa height | r850 |
| Near surface specific humidity | shum |
| *Geostrophic air flow velocity* | **_f |
| *Vorticity* | **_z |
| *Zonal velocity component* | **_u |
| *Meridional velocity component* | **_v |
| *Divergence* | **zh |
| ***Wind direction*** | **th |

*Table 2:* The squared Pearson correlation coefficient ($r^2$) between the monthly climatology of the NCEP/NCAR reanalysis and the HadCM3 climate model for the 77.5°N and 11.25°E grid-cell. Variables with $r^2 \geq 0.5$ are highlighted **bold** and are used for downscaling. See Table 1 for more details on the variable.

| Variable | $r^2$ | Variable | $r^2$ |
|---|---|---|---|
| mslp | 0.33 | p8_z | 0.28 |
| **p500** | **0.96** | p8zh | 0.07 |
| **p5_f** | **0.69** | **p5_f** | **0.95** |
| **p5th** | **0.59** | p5_th | 0.24 |
| **p5_u** | **0.67** | p5_u | 0.20 |
| **p5_v** | **0.75** | **p5_v** | **0.82** |
| p5_z | 0.01 | p5_z | **0.75** |
| **p5zh** | **0.77** | **p_zh** | **0.79** |
| **p850** | **0.86** | r500 | 0.11 |
| **p8_f** | **0.90** | r850 | 0.23 |
| **p8th** | **0.55** | rhum | 0.38 |
| **p8_u** | **0.71** | **shum** | **0.94** |
| p8_v | 0.03 | temp | **0.94** |

# 4 Results

## 4.1 Model Identification

The following sections summarise the results of the stepwise regression, used for model identification. For each variable (precipitation occurrence, precipitation intensity and temperature) a table showing the coefficients of the final model as well as the corresponding AIC is presented in combination with a figure illustrating the success of the best fit.

Table 3 shows the coefficients of the precipitation occurrence models (Eq. 1) for all catchments under consideration. Figure 2 compares the best estimate of the probability of precipitation occurrence to observed precipitation occurrences.

Table 4 shows the results of the stepwise regression used to identify the model for precipitation intensities (Eq. 3). Figure 3 compares the best fit predictions of precipitation intensities to the observed values. Note that the observations are limited to a resolution of 0.01 mm day$^{-1}$ which underlies the lined patterns.

Table 5 shows the coefficients of the daily temperature models (Equation 5) for all catchments under consideration and Figure 4 compares observed and fitted values.

## 4.2 Performance of weather generator

The following section assesses the ability of the conditional weather generator to capture important aspects of observed precipitation and temperature. For each variable in each catchment 1000 realisations where drawn, conditioned on the NCEP/NCAR reanalysis for the control period. The temporal evolution of these replicates corresponds to the observations and the spread of the simulations quantifies the uncertainty of the estimate.

The quality of the simulations is primarily assessed with focus on the mean annual cycle (i.e. the climatology), the monthly residuals (time series aggregated to monthly values with the longterm mean of each month removed) and the inter-annual variability. In addition, some attention is payed to the return periods of annual maxima and the autocorrelation function, both being relevant aspects of data that are available in daily resolution.

Beside visual comparisons, the performance of the weather generators is also assessed quantitatively.

*Table 3:* Coefficients of the best models for precipitation occurrence (Eq. 1) and the corresponding AIC for all considered catchments

| | Borgai | Eggedal | Holen | Langsima | Myrkdal | NoreEn | Sysima |
|---|---|---|---|---|---|---|---|
| Intercept | -0.51 | -0.45 | 0.06 | 0.21 | 0.24 | 0.40 | 0.28 |
| occurrence lag | 1.41 | 1.54 | 1.80 | 1.68 | 1.70 | 1.59 | 1.70 |
| p500 | -0.46 | -0.37 | -0.47 | -0.94 | -0.76 | -0.82 | -1.00 |
| p5_f | 0.30 | 0.27 | 0.35 | 0.40 | 0.47 | 0.35 | 0.45 |
| p5th | | | >0.01 | >0.01 | >0.01 | >0.01 | >0.01 |
| p5_u | -0.27 | -0.24 | 0.13 | 0.22 | 0.12 | | |
| p5_v | | | | 0.51 | | | 0.49 |
| p5zh | 0.39 | 0.43 | 0.43 | | 0.51 | 0.46 | |
| p850 | -0.40 | -0.41 | -0.30 | | | -0.23 | |
| p8_f | -0.23 | -0.19 | 0.16 | 0.14 | | | |
| p8th | | <-0.01 | >0.01 | >0.01 | | >0.01 | >0.01 |
| p8_u | -0.25 | -0.32 | 0.85 | 0.78 | 1.32 | 0.36 | 0.61 |
| p5_f | 0.46 | 0.42 | 0.17 | 0.27 | 0.19 | 0.46 | 0.47 |
| p5_v | -0.79 | -0.74 | | -0.20 | 0.36 | -0.22 | -0.54 |
| p_z | 0.45 | 0.43 | 0.50 | 0.35 | 0.44 | 0.36 | 0.39 |
| p5_zh | 0.86 | 0.76 | | | -0.52 | | 0.37 |
| shum | 0.75 | 0.63 | 0.71 | 0.75 | 0.77 | 0.88 | 0.84 |
| temp | -0.38 | -0.28 | -0.33 | -0.28 | -0.28 | -0.47 | -0.39 |
| AIC | 10702 | 10667 | 8023 | 7860 | 7680 | 7936 | 7805 |

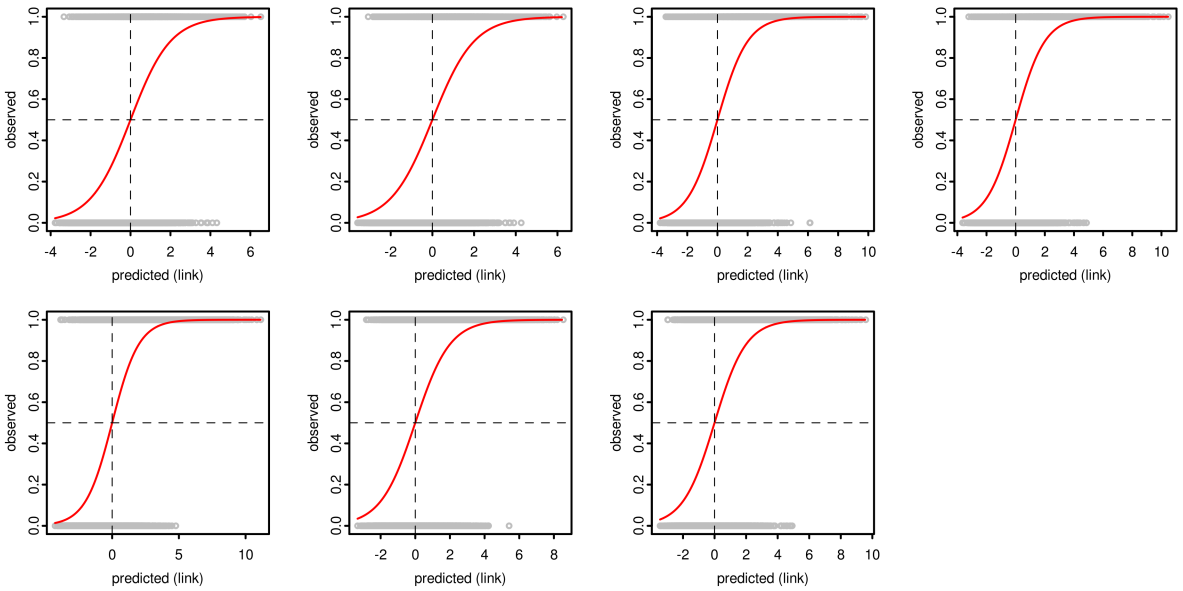


*Figure 2:* Best fit of the precipitation occurrence models. The x-axis shows the values predicted by Equation 1 (logistic transformation of the occurrence probability) and the y-axis shows observed precipitation occurrence (1 indicates a wet day). The red line is the inverse of the logistic transformation, mapping the predicted values onto the probability of precipitation occurrence (inverse of Equation 1).

*Table 4:* Coefficients of the best models for precipitation intensity (Eq. 3) and the corresponding AIC for all catchments considered

| | Borgai | Eggedal | Holen | Langsima | Myrkdal | NoreEn | Sysima |
|---|---|---|---|---|---|---|---|
| Intercept | 1.46 | 1.55 | 1.55 | 1.54 | 1.71 | 1.01 | 1.27 |
| p500 | | | | | | | |
| p5_f | 0.10 | 0.05 | 0.19 | 0.16 | 0.17 | 0.15 | 0.20 |
| p5th | | | <0.01 | <0.01 | | <0.01 | <0.01 |
| p5_u | -0.26 | -0.28 | 0.14 | 0.17 | 0.16 | | 0.07 |
| p5_v | 0.29 | 0.33 | 0.13 | | | | 0.13 |
| p5zh | | | | 0.18 | 0.22 | 0.30 | |
| p850 | -0.27 | -0.30 | -0.32 | -0.28 | -0.21 | -0.35 | -0.31 |
| p8_f | -0.07 | | | | | | |
| p8th | >-0.01 | >-0.01 | | | | | |
| p8_u | -0.08 | -0.07 | 0.43 | 0.42 | 0.52 | | 0.31 |
| p5_f | 0.12 | 0.11 | | 0.05 | 0.03 | 0.16 | 0.06 |
| p5_v | -0.44 | -0.51 | -0.20 | -0.21 | -0.21 | -0.12 | -0.18 |
| p5_z | 0.25 | 0.28 | 0.23 | 0.17 | 0.20 | 0.30 | 0.23 |
| p5_zh | 0.34 | 0.46 | | | | | |
| shum | 0.31 | 0.39 | 0.55 | 0.46 | 0.61 | 0.38 | 0.41 |
| temp | -0.18 | -0.29 | -0.49 | -0.32 | -0.53 | -0.29 | -0.33 |
| AIC | 29429 | 30940 | 43101 | 44484 | 44392 | 36806 | 41286 |

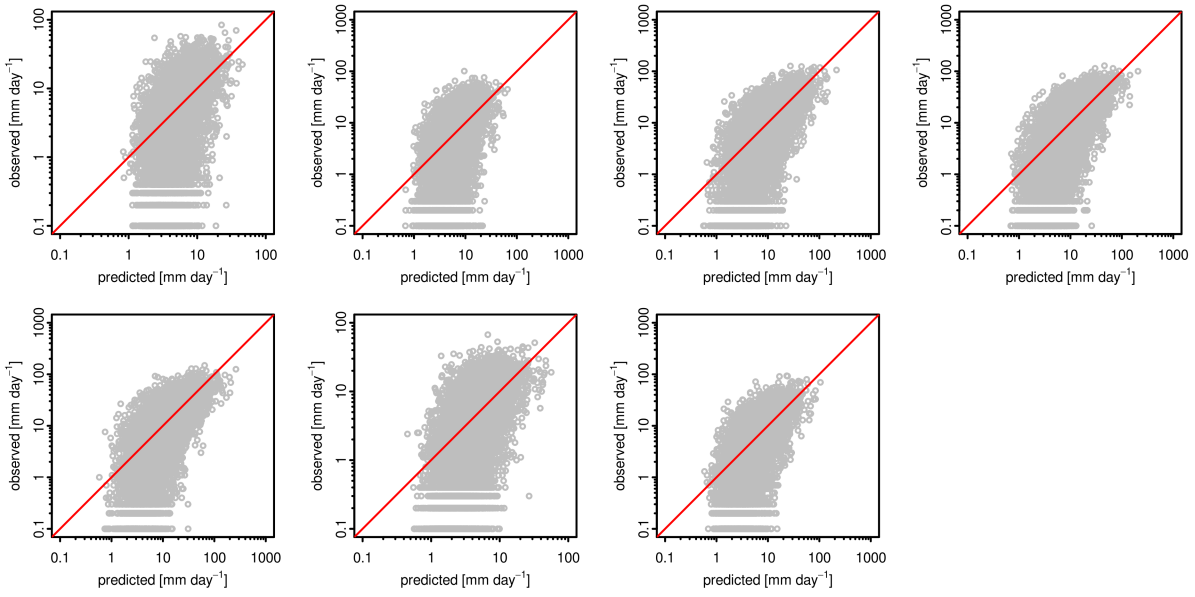


*Figure 3:* Best fit of the daily precipitation intensity model (Equation 3). The x-axis shows the best fit and the y-axis the observed intensities. The red line indicates equality.

*Table 5:* Coefficients of the best models for temperature (Eq. 5) and the corresponding AIC for all catchments considered

| | Borgai | Eggedal | Holen | Langsima | Myrkdal | NoreEn | Sysima |
|---|---|---|---|---|---|---|---|
| Intercept | -0.25 | 0.04 | -0.15 | -0.51 | 0.15 | -0.57 | -0.53 |
| temperature lag | 0.70 | 0.72 | 0.70 | 0.65 | 0.69 | 0.66 | 0.63 |
| p500 | 1.99 | 1.85 | 1.71 | 2.17 | 1.70 | 2.21 | 2.28 |
| p5_f | 0.11 | 0.11 | 0.04 | | | 0.05 | |
| p5th | | | <0.01 | | <0.01 | | |
| p5_u | -0.07 | | | -0.17 | -0.08 | -0.14 | -0.15 |
| p5_v | 0.58 | 0.60 | | | | 0.74 | 0.46 |
| p5zh | | | 0.36 | 0.49 | 0.43 | -0.22 | |
| p850 | -1.26 | -1.20 | -1.02 | -1.26 | -1.05 | -1.31 | -1.34 |
| p8_f | 0.45 | 0.43 | 0.34 | 0.42 | 0.34 | 0.48 | 0.46 |
| p8th | | | <0.01 | <0.01 | <0.01 | | |
| p8_u | -0.16 | -0.31 | -0.15 | 0.10 | -0.08 | | 0.07 |
| p_f | -0.21 | -0.19 | -0.05 | -0.16 | | -0.33 | -0.26 |
| p_v | -1.78 | -1.97 | -0.49 | -0.28 | -0.53 | -1.56 | -0.73 |
| p_z | 0.23 | 0.18 | 0.26 | 0.36 | 0.28 | 0.31 | 0.35 |
| p_zh | 1.01 | 1.17 | 0.21 | | 0.37 | 0.88 | 0.28 |
| shum | -0.37 | -0.36 | -0.16 | -0.23 | -0.33 | -0.38 | -0.24 |
| temp | 1.37 | 1.34 | 0.92 | 1.12 | 1.26 | 1.63 | 1.33 |
| AIC | 42380 | 42638 | 35232 | 37670 | 37182 | 39579 | 37836 |

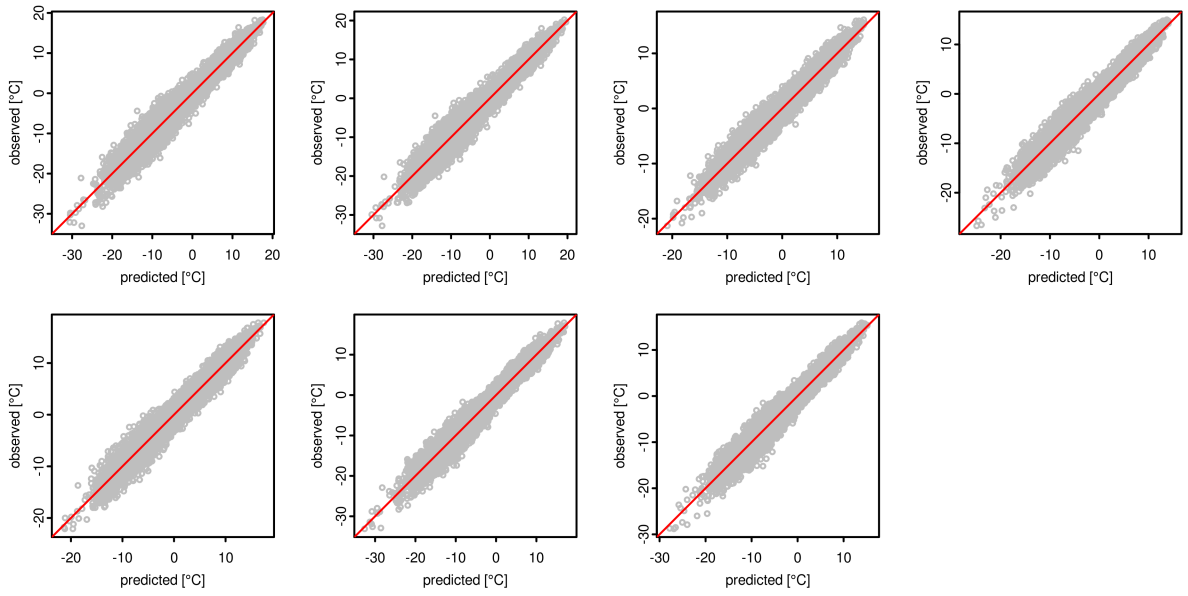


*Figure 4:* Best fit of the daily temperature model (Equation 5). The x-axis shows the best fit and the y-axis the observed temperatures. The red line indicates equality.

The bias is quantified using the mean difference between observed and simulated values (BIAS). The weather generators ability to capture different aspects of the temporal variability is quantified using the square of Pearson's correlation coefficient between the observed and the simulated mean annual cycle ($r^2_{Seas}$), monthly residuals ($r^2_{Resid}$) and annual values ($r^2_{Annual}$). The correlations are in every instance computed using the median of all simulations.

### 4.2.1 Precipitation

Table 6 quantifies the performance of the precipitation generator, i.e. the combined effect of simulated precipitation occurrence and precipitation intensity. For all catchments the model is almost unbiased with absolute value of the BIAS being well below 1 mm day$^{-1}$. The precipitation generator also captures the seasonality of precipitation reasonably well with all correlations ranging from $r^2_{Seas} = 0.85$ to $r^2_{Seas} = 0.96$. There is, however, a considerable spread in the simulated monthly climatology (Figure 5). The correlation between the observed and the simulated monthly precipitation residuals is lower ranging from $r^2_{Resid} = 0.56$ to $r^2_{Resid} = 0.85$. Notably, the spread of the simulations (indicated by the shaded areas in Figure 6) is small, compared to the magnitude of the variations in the median value. The lowest correlations are found for annual time series (Figure 7). Especially the large spread in the correlation coefficients, ranging from $r^2_{Annual} = 0.34$ to $r^2_{Annual} = 0.81$, is noteworthy and likely related to the fact that inter annual variability of precipitation is a weak signal.

Figure 8 compares the autocorrelation functions of observed and simulated daily precipitation for time lags up to 30 days. The autocorrelation of the simulated time series decays somewhat quicker than the autocorrelation of observed precipitation. This indicates that the weather generator underestimates the persistence of daily precipitation, despite the fact that the model for precipitation occurrence (Eq. 1) incorporates an autoregressive component.

Figure 9 compares the return periods of the annual maxima of simulated and observed precipitation. The weather generator dramatically overestimates the most extreme values, reaching unrealistic magnitudes.

*Table 6:* Performance of the precipitation generator forced with the NCEP/NCAR reanalysis

| | Borgai | Eggedal | Holen | Langsima | Myrkdal | NoreEn | Sysima |
|---|---|---|---|---|---|---|---|
| BIAS [mm day$^{-1}$] | <0.01 | 0.03 | 0.23 | 0.17 | 0.34 | 0.08 | 0.09 |
| $r^2_{Seas}$ | 0.85 | 0.86 | 0.92 | 0.95 | 0.92 | 0.92 | 0.96 |
| $r^2_{Resid}$ | 0.56 | 0.60 | 0.78 | 0.85 | 0.83 | 0.56 | 0.75 |
| $r^2_{Annual}$ | 0.38 | 0.53 | 0.67 | 0.81 | 0.80 | 0.34 | 0.53 |

### 4.2.2 Temperature

Table 7 summarises the performance of the weather generator for daily temperature on different time scales. The temperature simulations are effectively unbiased and the absolute values of the differences in mean and simulated temperatures are smaller than 0.01°C. The conditional weather generator captures the seasonality of precipitation very well with almost perfect correlations ($r^2_{Seas} \geq 0.97$). Further, the seasonality of the temperature simulations do have a very small spread (Figure 10). The weather generator also accurately simulates the monthly residuals of temperature. This is reflected by the relatively high correlation coefficients, which have a remarkably small spread, ranging from $r^2_{Resid} = 0.80$ to $r^2_{Resid} = 0.86$. The high degree of correlations is also reflected by the relatively small spread of the simulation around their median (Figure 11). The correlations of the observed and the simulated annual time series are only marginally lower than those found for the monthly residuals. Correlation coefficients range from $r^2_{Annual} = 0.76$ to $r^2_{Annual} = 0.84$. The spread of the model simulations is, comparatively large if compared to the magnitude of the inter-annual variability.

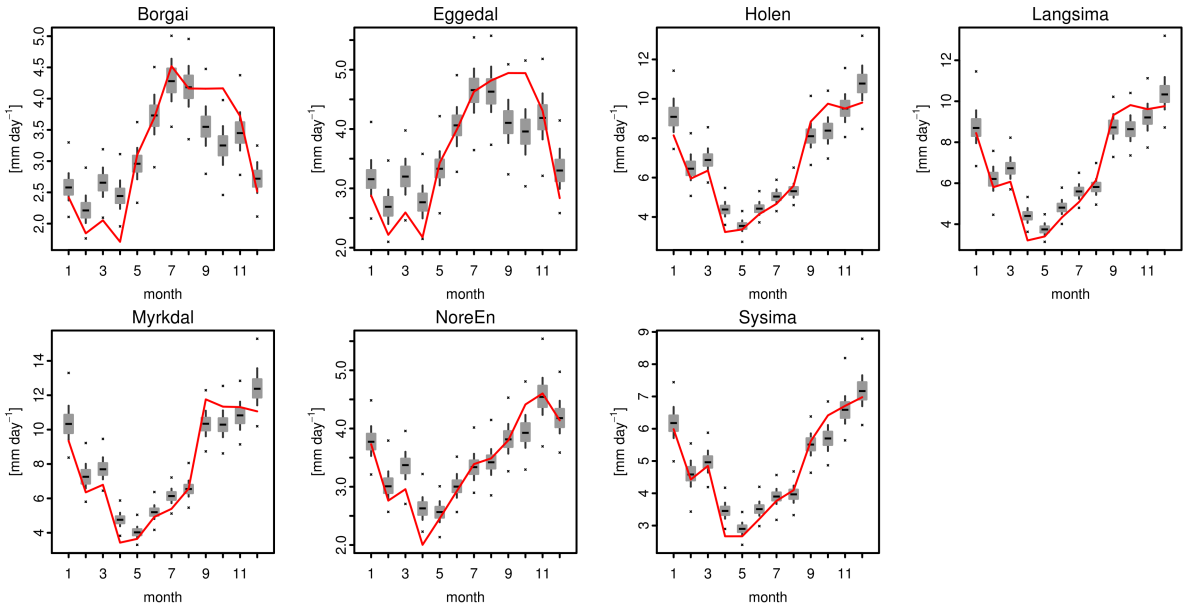


*Figure 5:* Observed (red lines) and simulated (boxplot) monthly precipitation climatologies. Boxes cover the interquartile range of the simulated monthly climatologies. The horizontal bar indicates the median. The whiskers range from the 10% to the 90% percentile. The dots indicate the lowest and the highest value of the simulations. The simulations where forced with the NCEP/NCAR reanalysis.

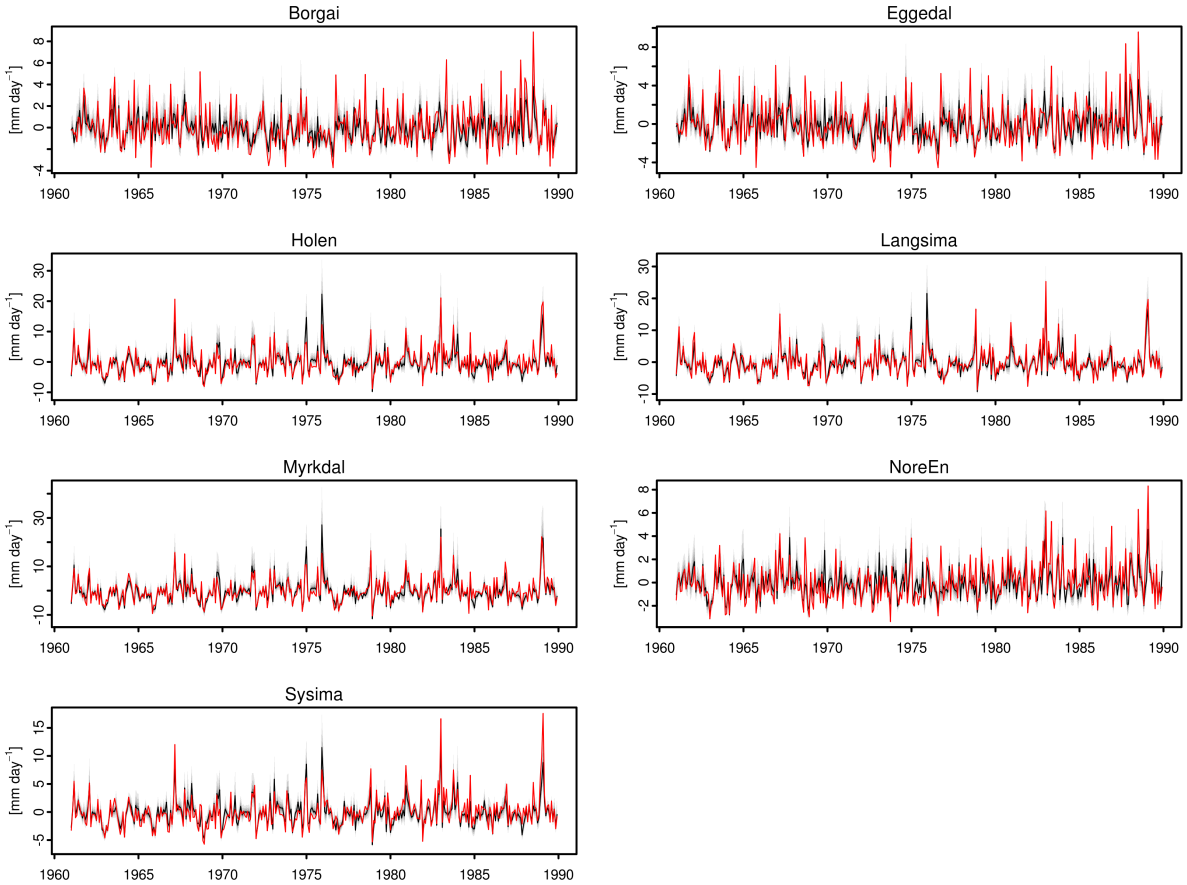


*Figure 6:* Comparison between observed and simulated monthly precipitation anomalies. Red line: observed value. The shaded areas are percentiles (10%, 20%, ..., 90%) of the simulation. The black line is the median (50% - percentile) of the simulation. The simulations where forced with the NCEP/NCAR reanalysis.

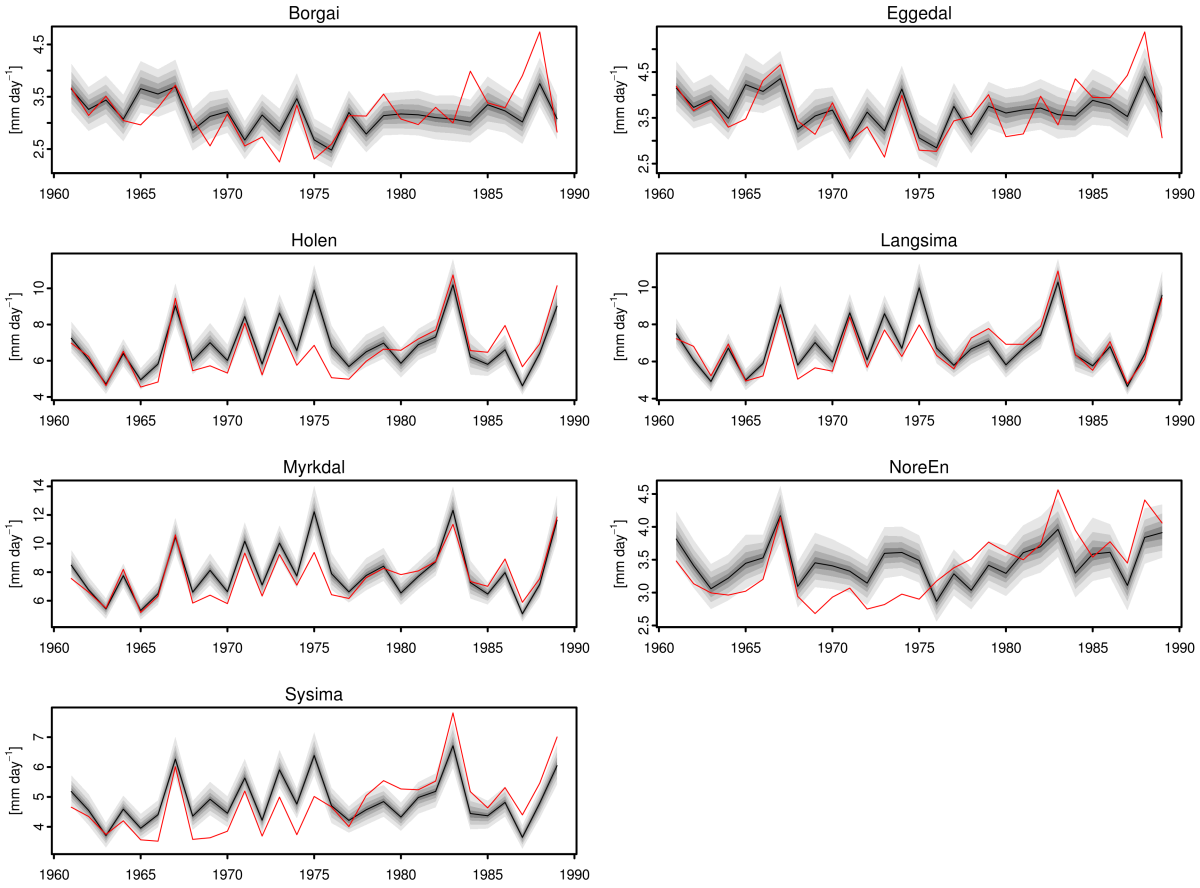


*Figure 7:* Comparing annual means of daily precipitation. Red line: observed value. The shaded areas are the percentiles (10%, 20%, ..., 90%) of the simulations forced with the NCEP/NCAR reanalysis. The black line is the median (50% - percentile) of the simulation.

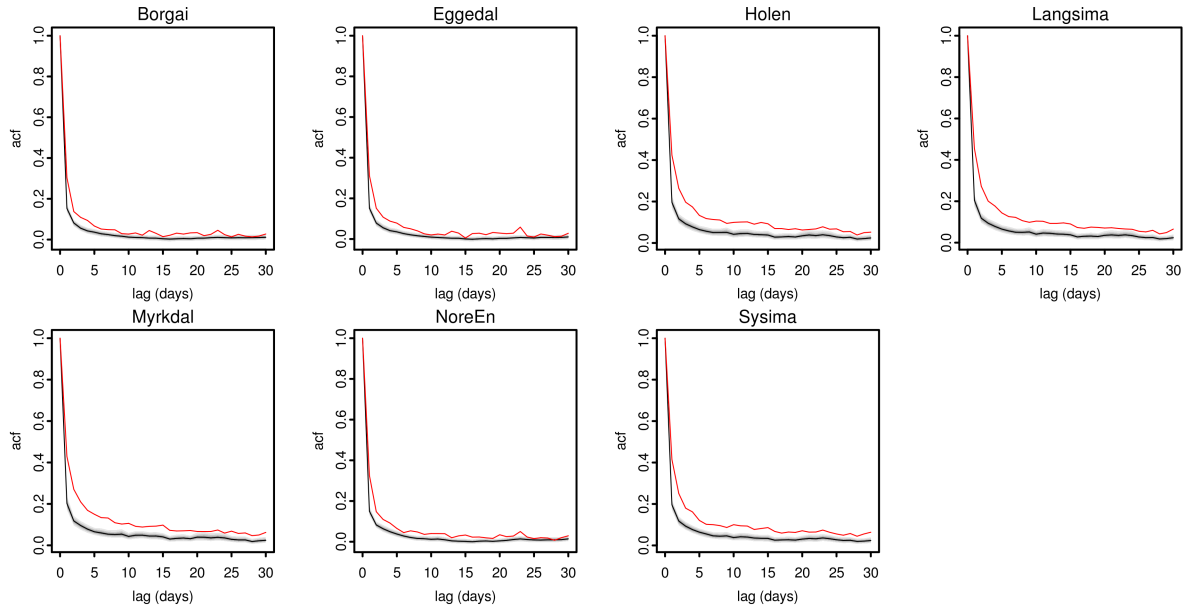


*Figure 8:* Autocorrelation function of daily precipitation. Red line: observed value. The shaded areas are the percentiles (10%, 20%, ..., 90%) of the simulations, forced with the NCEP/NCAR reanalysis. The black line is the median (50% - percentile) of the simulation.

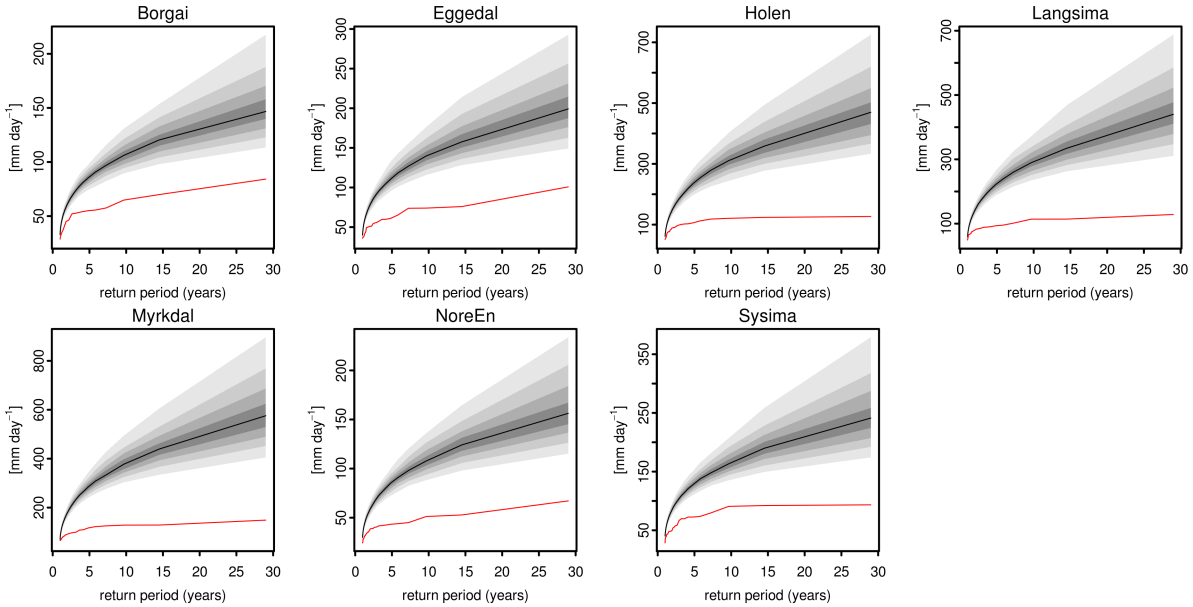


*Figure 9:* Return periods of annual maxima of observed and simulated precipitation. Red line: observed value. The shaded areas are percentiles (10%, 20%, ..., 90%) of the simulations, forced with the NCEP/NCAR reanalysis. The black line is the median (50% - percentile) of the simulation.

Figure 13 compares the autocorrelation functions of observed and simulated daily temperatures. The autocorrelation of both observed and simulated temperature exhibit a large degree of similarity and decay at approximately the same rate. The quality of the estimate is further supported by its comparatively small spread.

The return periods of the annual maxima of observed and simulated precipitation are compared in Figure 14. There is an overall tendency of the model to overestimate the magnitude of the most extreme values. In general, however, the estimated values maintain in a realistic range.

*Table 7:* Performance of the weather generator for daily temperature forced with the NCEP/NCAR reanalysis.

| | Borgai | Eggedal | Holen | Langsima | Myrkdal | NoreEn | Sysima |
|---|---|---|---|---|---|---|---|
| BIAS [°C] | >-0.01 | <0.01 | >-0.01 | <0.01 | >-0.01 | >-0.01 | >-0.01 |
| $r^2_{Seas}$ | 0.98 | 0.97 | 0.97 | 0.98 | 0.98 | 0.99 | 0.99 |
| $r^2_{Resid}$ | 0.81 | 0.80 | 0.82 | 0.86 | 0.84 | 0.85 | 0.86 |
| $r^2_{Annual}$ | 0.79 | 0.76 | 0.82 | 0.79 | 0.71 | 0.82 | 0.84 |

## 4.3 Climate Scenarios

The weather generators for precipitation and temperature have been used to downscale simulations of the HadCM3 climate model for the control and the scenario period. In the following the downscaled results of the HadCM3 model are first compared to observations and the downscaled NCEP/NCAR reanalysis with focus on the monthly climatology. Finally, the change in precipitation and temperature between the control and the scenario period is evaluated.

### 4.3.1 Perfromance of the downscaled Climate Model

Table 8 quantifies the skill of the downscaled HadCM3 model to capture the monthly precipitation climatology. The bias does not exceed 0.17 mm day$^{-1}$ and has an order of magnitude that is comparable to the simulations forced with the NCEP/NCAR reanalysis (Table 6). The correlation between the observed precipitation climatology and the climatology of the simulations forced with the HadCM3 model

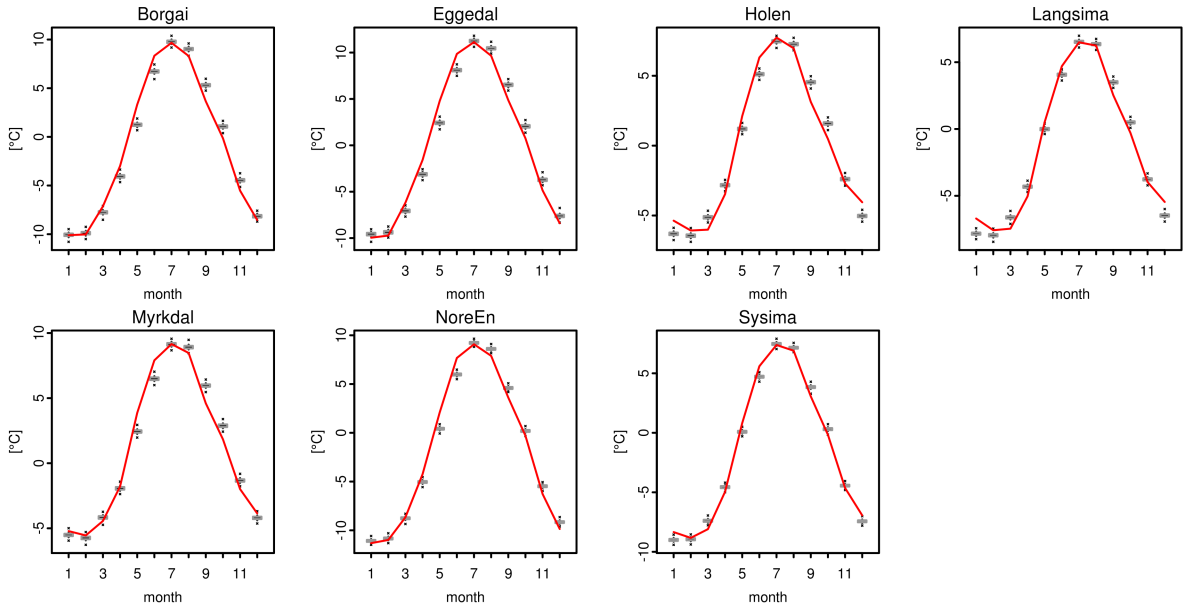


*Figure 10:* Observed (red lines) and simulated (boxplot) monthly temperature climatologies. Boxes cover the inter-quartile range of the simulated monthly climatologies. The horizontal bar indicates the median. The whiskers range from the 10 to the 90 percentile. The points indicate the lowest and the highest value of the simulations. The simulations where forced with the NCEP/NCAR reanalysis.

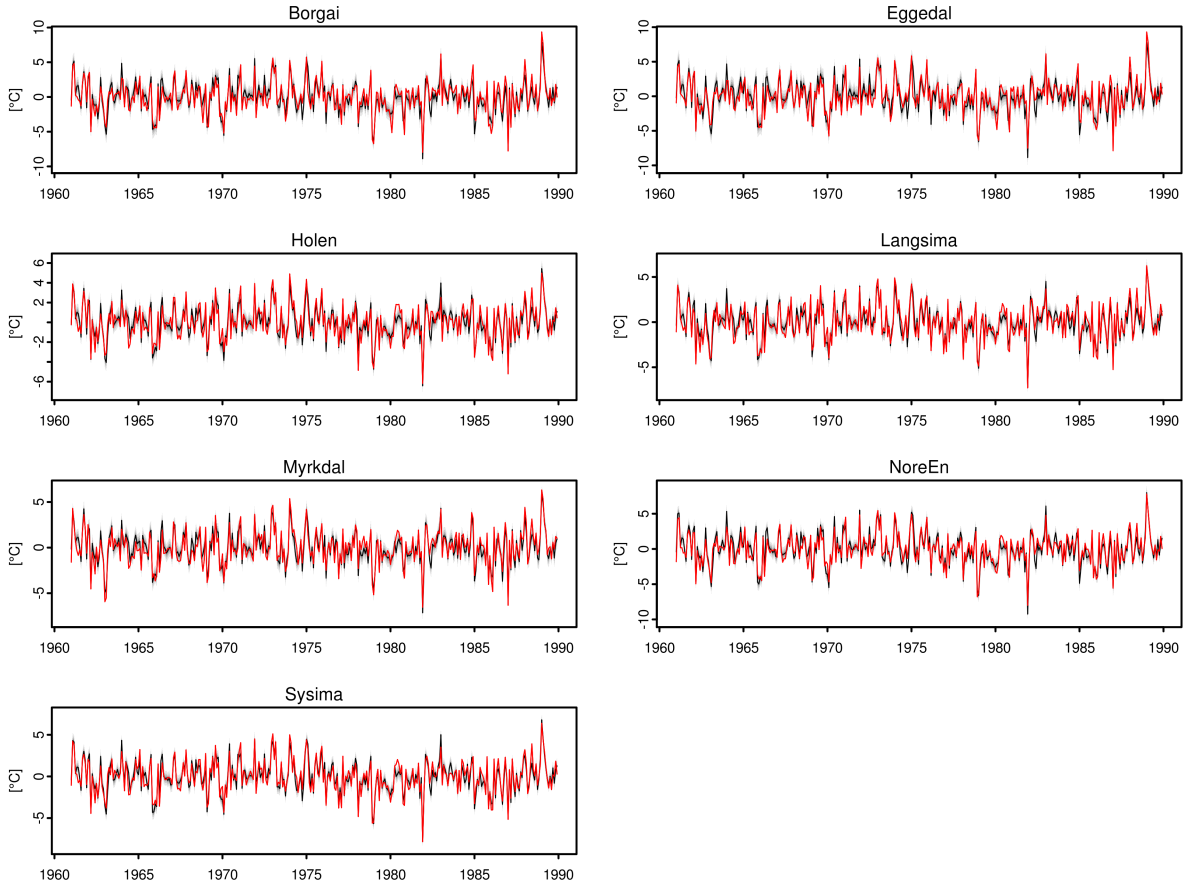


*Figure 11:* Comparison between observed and simulated monthly temperature anomalies. Red line: observed value. The shaded areas are the percentiles (10%, 20%, ..., 90%) of the simulations, forced with the NCEP/NCAR reanalysis. The black line is the median (50% - percentile) of the simulation.

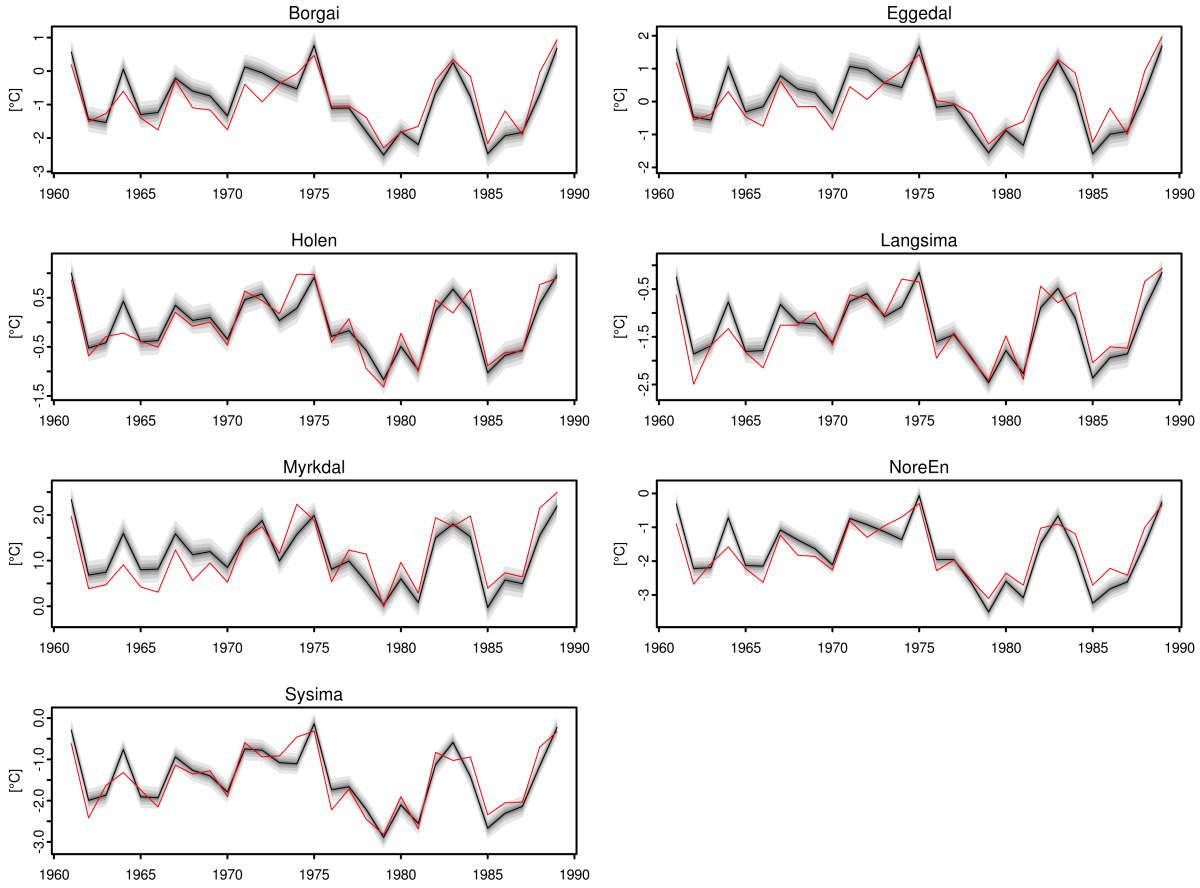


*Figure 12:* Comparing time series of annual mean temperature. Red line: observed value. The shaded area are the percentiles (10%, 20%, ..., 90%) of the simulations, forced with the NCEP/NCAR reanalysis. The black line is the median (50% - percentile) of the simulation.

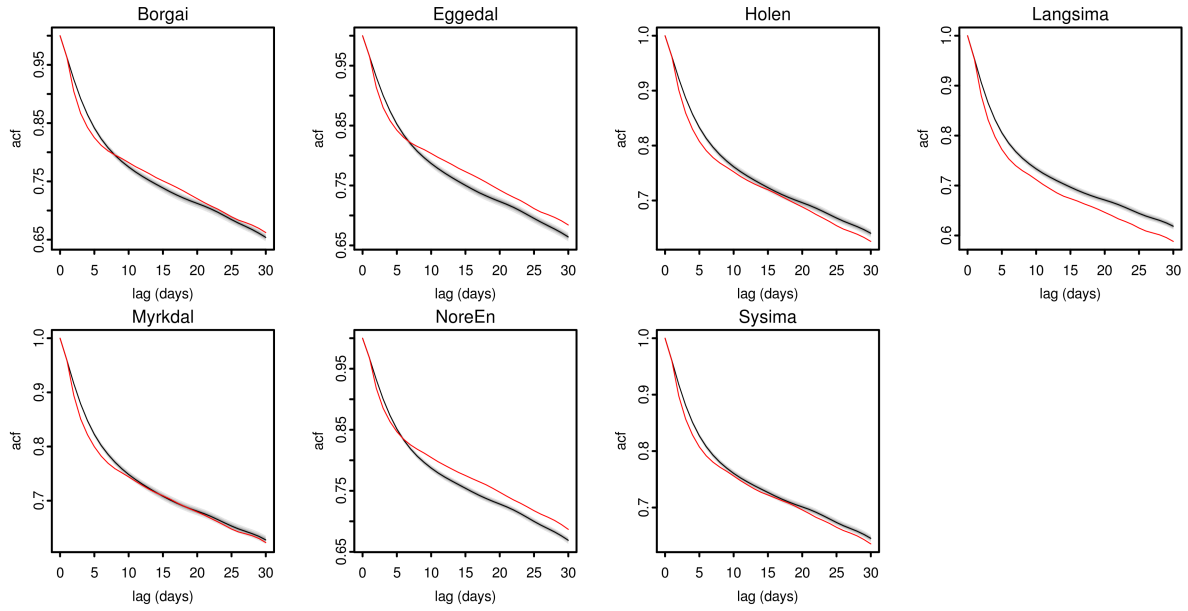


*Figure 13:* Autocorrelation function of daily temperature. Red line: observed value. The shaded areas are the percentiles (10%, 20%, ..., 90%) of the simulations, forced with the NCEP/NCAR reanalysis. The black line is the median (50% - percentile) of the simulation.

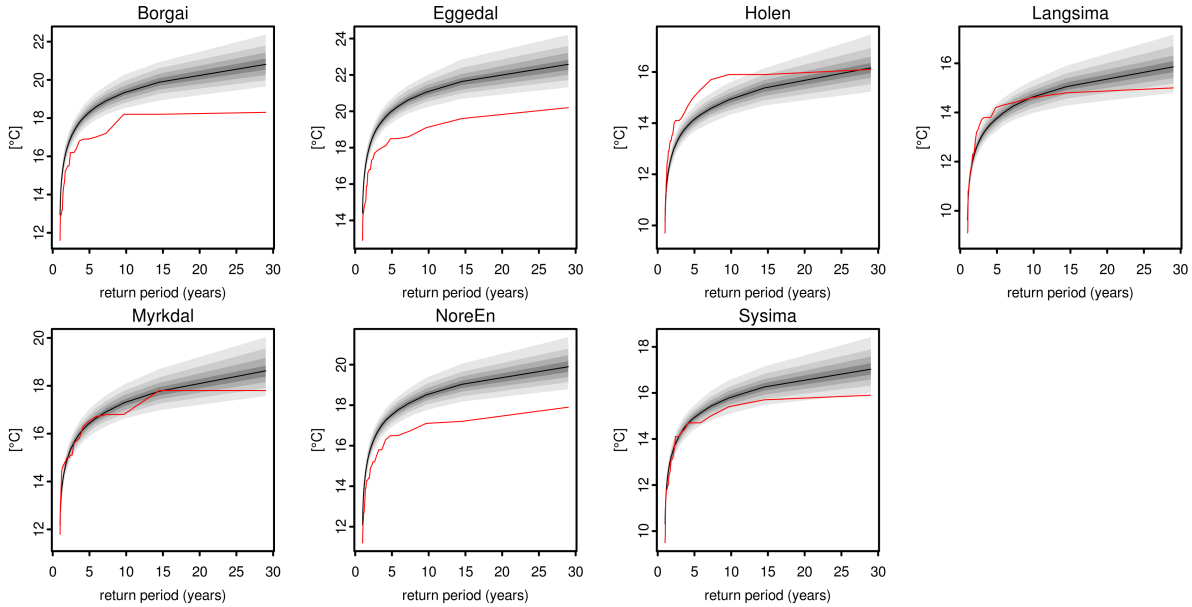


*Figure 14:* Return periods annual maxima of observed and simulated daily temperature. Red line: observed value. The shaded areas are the percentiles (10%, 20%, ..., 90%) of the simulations, forced with the NCEP/NCAR reanalysis. The black line is the median (50% - percentile) of the simulation.

ranges from $r^2_{Seas} = 0.16$ to $r^2_{Seas} = 0.55$, which is substantially lower than the correlations found for the simulations forced with the NCEP/NCAR reanalysis. Figure 15 compares the observed precipitation climatology with the climatologies resulting from downscaling the NCEP/NCAR and the HadCM3 reanalysis. This illustration suggests that some of the largest deviations between the simulations forced with NCEP/NCAR and the simulations forced with the HadCM3 occur during the autumn and winter months. The error can be characterised by an underestimation of the HadCM3 simulations in the late autumn which is subsequently followed by an overestimation in early spring.

Table 9 quantifies the skill of the downscaled HadCM3 model to capture the mean annual cycle of temperature. The bias is never exceeding 0.1°C but is slightly larger than the bias of the NCEP/NCAR based simulations (Table 7). The correlations between the mean annual cycle of observed temperature and the HadCM3 based temperature simulations is very high and comparable to the ones found for the simulations forced with NCEP/NCAR. Figure 16 compares the observed mean annual cycles of temperature with the NCEP/NCAR as well as the HadCM3 based simulations. The similarity of all three quantities visually supports the results of the correlation analysis.

*Table 8:* Performance of the precipitation generator forced with the HadCM3 model in the control 1961 - 1990 period.

| | Borgai | Eggedal | Holen | Langsima | Myrkdal | NoreEn | Sysima |
|---|---|---|---|---|---|---|---|
| BIAS [mm day$^{-1}$] | 0.11 | 0.13 | 0.02 | 0.11 | 0.17 | 0.17 | 0.04 |
| $r^2_{Seas}$ | 0.33 | 0.20 | 0.52 | 0.57 | 0.55 | 0.16 | 0.51 |

*Table 9:* Performance of the weather generator for temperature forced with the HadCM3 model in the 1961 - 1990 control period

| | Borgai | Eggedal | Holen | Langsima | Myrkdal | NoreEn | Sysima |
|---|---|---|---|---|---|---|---|
| BIAS [mm day$^{-1}$] | 0.07 | 0.08 | 0.09 | 0.09 | 0.10 | 0.07 | 0.06 |
| $r^2_{Seas}$ | 0.99 | 0.99 | 0.97 | 0.96 | 0.98 | >0.99 | 0.98 |

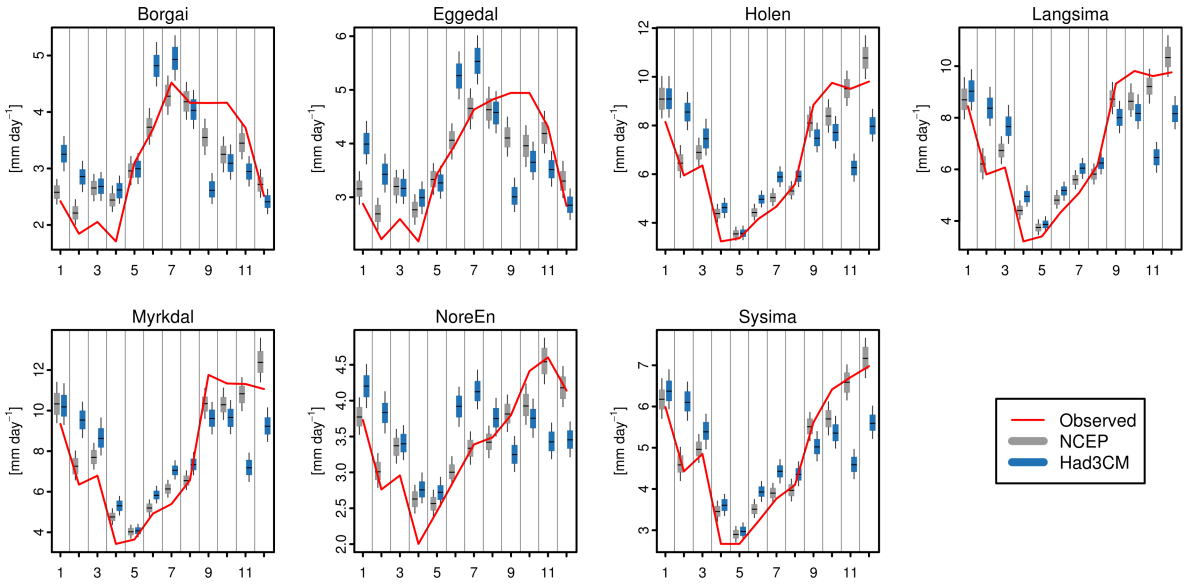


*Figure 15:* Observed precipitation climatology compared to downscaled results based on the NCEP/NCAR reanalysis and the HadCM3 climate model for the 1961 - 1990 control period. Boxes cover the inter-quartile range of the simulated monthly climatologies. The horizontal bar indicates the median. The whiskers range from the 10% to the 90% percentile.

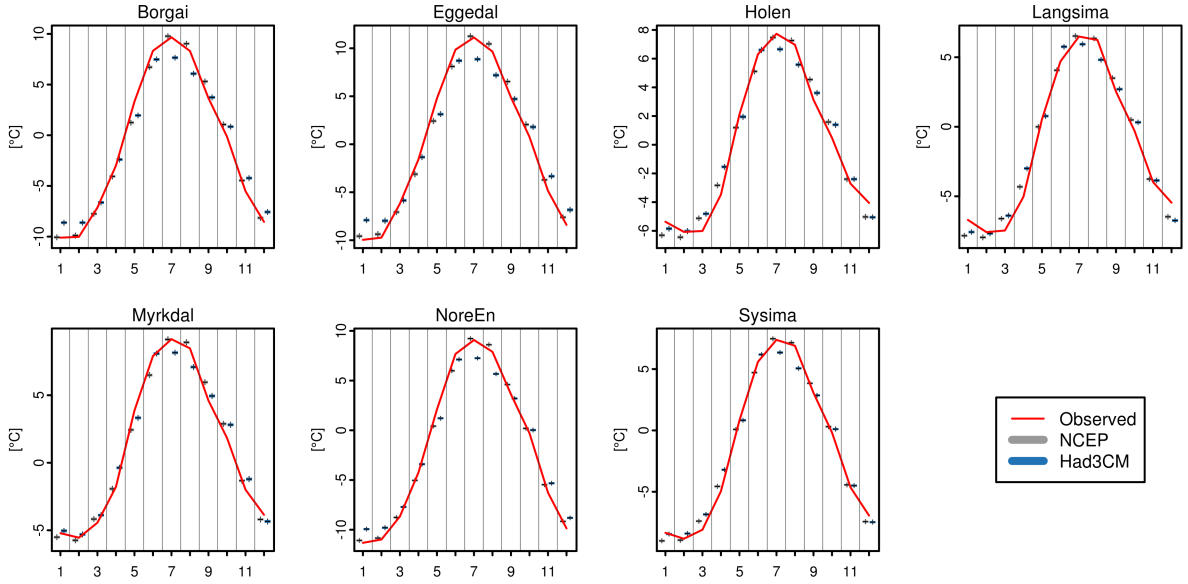


*Figure 16:* Observed temperature climatology compared to downscaled results based on the NCEP/NCAR reanalysis and the HadCM3 climate model for the 1960 - 1990 control period. Boxes cover the inter-quartile range of the simulated monthly climatologies. The horizontal bar indicates the median. The whiskers range from the 10% to the 90% percentile.

### 4.3.2 Projected Changes in Precipitation and Temperature

To assess the effects of climate change on precipitation and temperature the difference of the monthly climatology between the scenario (1971 - 2100) and the control period (1961 - 1990) has been evaluated. To judge upon the reliability of the projections the absolute change was compared to the median absolute error (MAE) for each month. The MAE is defined as the median of the absolute values of the difference between the observed climatology and the climatology of each of the 1000 simulations. The projected changes are considered reliable only if 75% of the simulations have changes with absolute values larger than the MAE (i.e. the boxes in Figure 17 and 18 have to be completely outside the area covered by $\pm$MAE).

Figure 17 shows the projected changes in precipitation for both the A2 and the B2 emission scenario. In Holen, Langsmia, Myrkedal and Sysmia an increase in precipitation is projected for the late summer and early autumn months, which is more pronounced for the A2 emission scenario. Notably these catchments are also the catchments where the simulations forced with HadCM3 exhibit the highest skill in the control period (see Table 8). This, together with a tendency of decreasing precipitation in spring, suggests a change in the seasonality of precipitation with dryer conditions in late winter and spring opposed by increasingly wet conditions in late summer and early autumn.

Figure 18 illustrates the changes in temperature. In contrast to precipitation, the projected changes are in most cases larger than the MAE and point toward warming condition. The projections that are based on the A2 scenario are consistently about two degrees warmer than the ones that are based on the B2 scenario. The systematic increase in temperature implies in combination with the observed climatology (Figure 10 and 16) a considerably shorter frost season for both emission scenarios.

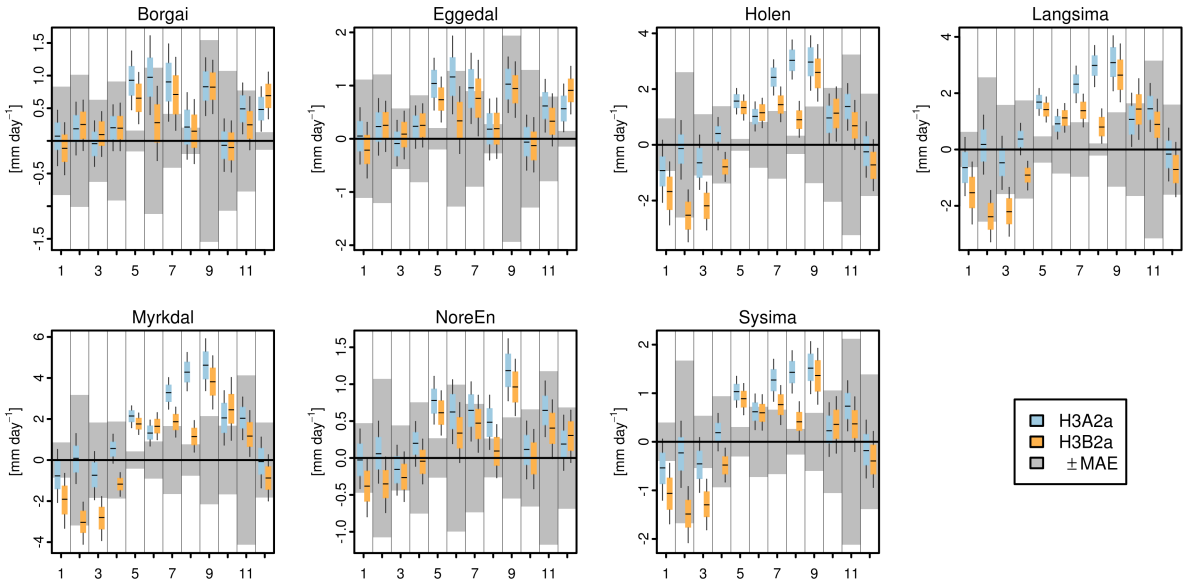


*Figure 17:* Projected changes in mean precipitation rate, quantified as the difference in the monthly climatology between the scenario (1961 - 1990) and the control period (2071 - 2100). H3A2a: HadCM3 model forced with the A2 emission scenario. H3B2a: HadCM3 model forced with the B2 emission scenario. MAE: median absolute error between the observed and the simulated climatology for each month.

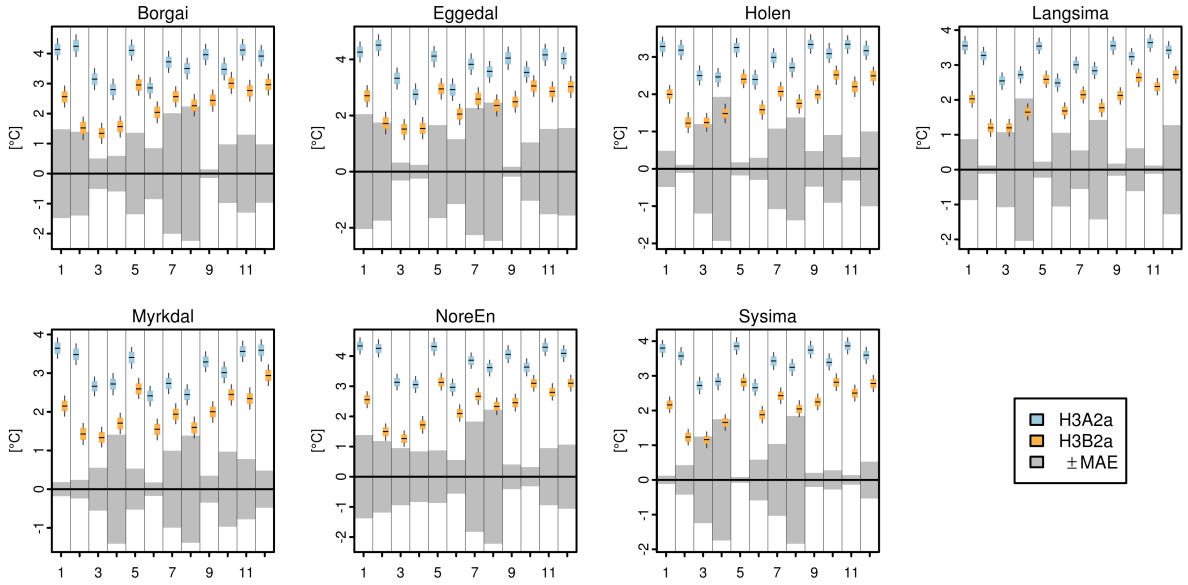


*Figure 18:* Projected changes in mean temperature, quantified as the difference in the monthly climatology between the scenario (1961 - 1990) and the control period (2071 - 2100). H3A2a: HadCM3 model forced with the A2 emission scenario. H3B2a: HadCM3 model forced with the B2 emission scenario. MAE: median absolute error between the observed and the simulated climatology for each month.

# 5 Summary and Conclusions

## 5.1 Verdict of the GLM based weather generator

The primary aim of this study was to assess the ability of conditional weather generators to capture important aspect of precipitation and temperature variability. The chosen approach was based on using relatively simple stochastic simulators with time varying parameters (e.g. the probability of precipitation occurrence). The value of these time varying parameters is dependent on free-atmosphere variables and was modelled on a day to day basis using Generalised Linear Models (GLM). The use of GLM allowed for an effective model identification using stepwise multiple regression in a maximum likelihood framework.

The GLM based weather generators for precipitation and temperature proved to be powerful tools, that successfully captured many aspects of precipitation and temperature variability. Most relevant are the ability to capture the mean annual cycle as well as monthly variability. Both aspects where described well for both precipitation and temperature. The fact that the temperature simulations had the edge over the precipitation simulations is most likely related to the more complex temporal structure of daily precipitation.

The situation differs slightly for the annual variability. Here, the temperature simulations clearly outperform the precipitation simulations. The reasons for this are not fully understood, but may be related to the fact that the inter-annual variability of precipitation is weak if compared to the inter-annual variability of temperature.

One of the most important aspects of daily precipitation and temperature is the degree of dependence between adjacent days. Both the precipitation and the temperature model explicitly account for this, by incorporating a first order autoregressive (Markov) component. Further, some degree if temporal dependence is introduced implicitly by the atmospheric forcing variables. The fact that both the precipitation and the temperature simulations captured the autocorrelation functions of the observations reasonably well proves the capability of the weather generators to describe short term persistence of the observed time series.

Extremely high values of precipitation and temperature regularly gain a lot of attention, for example with respect to floods and heat waves. As weather generators produce estimates of both variables with a daily resolution it is natural to check whether the magnitude and the return periods of the most extreme events is captured. Unfortunately, the weather generators used in this study overestimate the magnitude of the annual maxima. Especially for precipitation, where unrealistically high values are reached. Therefore, the present approach should not be used to assess the influence of climate change on extreme events. This is not completely unexpected. Similar issues of comparable downscaling techniques with respect to extremes have been previously reported and solutions to this issue, based on extreme value theory have been suggested. The review of Maraun et al. (2010) comments on this issue and provides references to guide further reading.

## 5.2 Suitability for climate projections

In the context of climate projections, the reliability of conditional weather generators does not only depend on the weather generator it self but also on the ability of the forcing model to capture the observed climatology. Therefore, it is not surprising that the performance of the weather generator decreased once it was forced with the HadCM3 model, despite the fact that forcing variables with a low skill where excluded form the analysis. (It should be noted that a more rigorous criterion for preselecting the forcing variables did not lead to increased skill of the weather generator if forced with the HadCM3 model, although this is not shown in this report.)

This issue highlights the secondary role of statistical weather-generators as post-processing (or downscaling) tools in climate impact research. The climate signal is computed by global climate models, which

consequently have the strongest impact on the reliability of the estimated change. This issue can in principle be approached by exploiting the fact that climate models are often more skillful with respect to specific variables. This knowledge can in principle be considered by more advanced data preprocessing or be incorporated into the procedure used to identify the statistical model.

## 5.3 Considerations for hydrological modelling

Conditional weather generators are often used to provide hydrological models with estimates of daily precipitation and temperature for climate impact assessment. Therefore it is important that weather generators do not only provide reliable estimates of the precipitation and temperature climatology, but also produce a realistic day to day variability. The stochastic nature of weather generators, however, renders a direct interpretation of simulated daily values unreliable. Hence, statistical summaries that give insights to selected aspects of the daily variability were used to asses the realism of the simulations. In the context of hydrological modelling the persistence, i.e. the degree of dependence between consecutive days, is often considered to be crucial. The close proximity between the autocorrelation function of observations and simulations for both precipitation and temperature (Figure 8 and Figure 13) indicated that this criterion was met. However, a series of issues regarding the daily variability of precipitation arose in this particular study. The relatively low predictive skill of daily precipitation intensity (Figure 3) and the fact that annual maxima are overestimated (Figure 9) may compromise hydrological applications. Therefore the suitability of conditional weather generators for hydrological modelling requires further investigation and will most likely depend on the needs of each specific study.

A possibly practical limitation of conditional weather generators in hydrological modelling is related to computational resources. The stochastic nature of weather generators implies that single realisations should not be interpreted and reliable applications always depend on a large number (> 1000) of replicates. However, the computational effort to process these with hydrological models may be unfeasible in many instances.

## 5.4 Hydrological implications of projected change

The uniform increase in temperature found for the A2 and the B2 emission scenario, irrespective the considered catchment, is likely to systematically alter the seasonality of hydrological phenomena. In the summer months, the increasing temperature will lead to increasing evapotranspiration rates, which may lead to dryer conditions. However, increasing evapotranspiration can trigger more convective rainfall - a phenomenon that cannot be resolved by the statistical model underlying this study. More dramatic may be the impact of the increasing temperature in the cold season. In all catchments considered mean monthly temperature is below zero for six months in the cold half of the year. Precipitation falling in these months is stored as snow, leading to low availability of liquid water during winter and an pronounced spring flood during snow melt. Increasing temperatures will shorten the snow period considerably and consequently alter the seasonality of most hydrological variables including river flow. The effects of temperature of the seasonality of hydrological variables is supplemented with weak changes in the seasonality of precipitation. The tendency for increasing precipitation in the late summer months with a simultaneous decrease in precipitation during late winter implies that less precipitation is stored as snow in the shortening frost season.

# References

Fealy, R. and J. Sweeney, 2007: Statistical downscaling of precipitation for a selection of sites in Ireland employing a generalised linear modelling approach. *International Journal of Climatology*, **27 (15)**, 2083–2094, doi:10.1002/joc.1506.

Fowler, H. J., S. Blenkinsop, and C. Tebaldi, 2007: Linking climate change modelling to impacts studies: recent advances in downscaling techniques for hydrological modelling. *International Journal of Climatology*, **27 (12)**, 1547–1578, doi:10.1002/joc.1556.

Furrer, E. M. and R. W. Katz, 2007: Generalized linear modeling approach to stochastic weather generators. *Climate Research*, **34 (2)**, 129–144, doi:10.3354/cr034129.

Hessami, M., P. Gachon, T. B. Ouarda, and A. St-Hilaire, 2008: Automated regression-based statistical downscaling tool. *Environmental Modelling & Software*, **23 (6)**, 813 – 834, doi:10.1016/j.envsoft.2007.10.004.

Maraun, D., et al., 2010: Precipitation downscaling under climate change: Recent developments to bridge the gap between dynamical models and the end user. *Rev. Geophys.*, **48 (3)**, RG3003, doi:10.1029/2009RG000314.

Wilby, R., L. Hay, and G. Leavesley, 1999: A comparison of downscaled and raw GCM output: implications for climate change scenarios in the San Juan River basin, Colorado. *Journal of Hydrology*, **225 (1-2)**, 67 – 91, doi:10.1016/S0022-1694(99)00136-5.

Wilby, R. L. and C. W. Dawson, 2007: *SDSM 4.2 – A decision support tool for the assessment of regional climate change impacts*.

Wilks, D. S. and R. L. Wilby, 1999: The weather generation game: a review of stochastic weather models. *Progress in Physical Geography*, **23 (3)**, 329–357, doi:10.1177/030913339902300302.

Winkler, J. A., G. S. Guentchev, M. Liszewska, Perdinan , and P.-N. Tan, 2011a: Climate Scenario Development and Applications for Local/Regional Climate Change Impact Assessments: An Overview for the Non-Climate Scientist - Part II: Considerations When Using Climate Change Scenarios. *Geography Compass*, **5 (6)**, 301–328, doi:10.1111/j.1749-8198.2011.00426.x.

Winkler, J. A., et al., 2011b: Climate Scenario Development and Applications for Local/Regional Climate Change Impact Assessments: An Overview for the Non-Climate Scientist - Part I: Scenario Development Using Downscaling Methods. *Geography Compass*, **5 (6)**, 275–300, doi:10.1111/j.1749-8198.2011.00425.x.